

Fluorescent Boron Bis(phenolate) with Association Response to Chloride and Dissociation Response to Fluoride

Ewan Galbraith,[†] Thomas M. Fyles,[‡] Frank Marken,[†] Matthew G. Davidson,^{*†} and Tony D. James^{*†}

Department of Chemistry, University of Bath, Bath BA2 7AY, U.K., and Department of Chemistry, University of Victoria, Victoria BA2 7AY, Canada

Received February 8, 2008

Addition of chloride ions to boron bis(phenolate) **5** in dichloromethane solution produces a selective fluorescence decrease. The fluorescence change is believed to be caused by associative hydrogen bonding between the chloride ion and two boronic acid groups. While addition of fluoride ions to bis(phenolate) **5** generates a purple colorimetric response, the colorimetric response is caused by fluoride induced B–O bond cleavage and air oxidation of the phenolate anion formed by this dissociation.

Introduction

An increasing amount of research effort has been devoted to the design and development of novel chemosensors for anions.¹ Anion sensor design poses a greater challenge to chemists than the more established field of cation sensors. Anions are larger than their respective isoelectronic cations and hence possess a lower charge to radius ratio, meaning any electrostatic binding interactions are less effective. Anions possess a high solvation energy and protonation of anions at low pH can also be an issue, so receptors have to operate within a useful pH range. Another challenge to overcome is that anionic species are not restricted to simple geometry, for example, trigonal planar carboxylate and tetrahedral phosphate ions. Hydroxylic solvents are able to form strong hydrogen bonds with anions, and so a sensor may also have to successfully compete with any such interactions.

Anion recognition can be achieved via a number of different noncovalent binding modes. Electrostatic interactions, which have the inherent drawback of the presence of a competing counterion, can be used alone or cooperatively with hydrogen bonding interactions. The directionality of hydrogen bonding can allow receptors of a complementary shape to the target anion to be designed, allowing differentiation between various guest species. Electron-deficient Lewis

acid coordination via orbital overlap has received a lot of attention, and receptors containing boron² (our particular focus), silicon,³ tin,^{4,5} and mercury⁶ have all emerged.

The anion recognition or binding event is most often transduced into an optical or electrochemical response. A chromogenic response is attractive from a qualitative point of view, in that a naked-eye visualization of the presence of a target anion avoids spectroscopy or any other analysis. Phosphorescence has seen limited use, with fluorescence being the most widespread signaling method.

Fluorescence is an excellent method of communicating a recognition event. The ability to relay information remotely, for example, from within living tissue, widens the potential of a fluorescent sensor for practical use. Response in the submillisecond time frame is achievable, and active fluorophores can be located with subnanometer accuracy, allowing real-time, real-space monitoring.⁷

Sensitivity is another attractive aspect of using fluorescent systems, with single guest molecule recognition being observable with the use of modern instrumentation.⁸ The

* To whom correspondence should be addressed. E-mail: m.g.davidson@bath.ac.uk (M.G.D.), t.d.james@bath.ac.uk (T.D.J.).

[†] University of Bath.

[‡] University of Victoria.

(1) Sessler, J. L.; Gale, P. A.; Cho, W. S. *Anion Receptor Chemistry*; Royal Society of Chemistry: London, 2006.

(2) Yamaguchi, S.; Akiyama, S.; Tamao, K. *J. Am. Chem. Soc.* **2001**, *123*, 11372–11375.

(3) Tamao, K.; Hayashi, T.; Ito, Y. *J. Organomet. Chem.* **1996**, *506*, 85–91.

(4) Newcomb, M.; Blanda, M. T.; Azuma, Y.; Delord, T. J. *J. Chem. Soc., Chem. Commun.* **1984**, 1159–1160.

(5) Newcomb, M.; Madonik, A. M.; Blanda, M. T.; Judice, J. K. *Organometallics* **1987**, *6*, 145–150.

(6) Yang, X.; Knobler, C. B.; Hawthorne, M. F. *Angew. Chem., Int. Edit. Engl.* **1991**, *30*, 1507–1508.

(7) Bissell, R. A.; de Silva, A. P.; Gunaratne, H. Q. N.; Lynch, P. L. M.; Maguire, G. E. M.; Sandanayake, K. R. A. S. *Chem. Soc. Rev.* **1992**, *21*, 187–195.

(8) Sauer, M. *Angew. Chem., Int. Edit.* **2003**, *42*, 1790–1793.

impact on the system undergoing analysis is minimal as concentrations are typically in the order of 10^{-6} M. This efficiency combined with the versatility of fluorescent sensors has led to several commercial uses, including point-of-care diagnostic monitoring and blood gas analysis in hospitals.^{9,10}

Fluoride is the smallest anion, with a high charge density and a hard Lewis basic nature that result in unusual chemical properties. The determination of the presence of fluoride is not merely an interesting academic challenge, with fluoride having an important role in a diverse array of biological, medical, and technological processes applications.

It has been well documented for some time that fluoride plays an important role in dental health,¹¹ and a great deal of interest has focused on its potential in treatment of osteoporosis.^{12,13} Fluoride is easily absorbed but is excreted slowly from the body, which can result in chronic poisoning. Overexposure to fluoride can lead to acute gastric and kidney problems.¹⁴ In several Less Economically Developed Countries excess fluoride levels in drinking water has been linked to fluorosis, a debilitating bone disease. UNICEF estimates that "fluorosis is endemic in at least 25 countries across the globe. The total number of people affected is not known, but a conservative estimate would number in the tens of millions." Hazardous levels may be as low as 1 ppm, requiring sensitive detection.

Fluoride detection is important in a number of military applications. The refinement of uranium in nuclear weapons manufacture requires fluoride monitoring.¹⁵ GB, more commonly known as Sarin (isopropyl methylphosphonofluoridate) was the nerve agent employed by the Aum Shinrikyu cult in the terrorist attacks that occurred in Tokyo in 1995. Fluoride is a product of hydrolysis of Sarin (and Soman, a related G-type agent), and the ability to monitor fluoride exposure of victims and the surrounding environment after an incident would be of great value.^{16,17}

As a result of this diversity, the development of sensitive and selective methods of fluoride detection under environmental conditions has been of particular focus in the field of anion recognition. It is also relevant to note the medical emphasis of the need for a fluoride sensor, reiterating fluorescence as a desirable signaling method because of the potential for intracellular use.

Chloride (usually from sodium chloride) is essential for human health, regulating blood pressure, maintaining metabolism and the acid–base balance within the body. Typical levels are at around 0.1 M in blood serum. High (hyper-

chloremia) and low (hypochloremia) levels of chloride can be dangerous and are often indicative of kidney problems. Chloride in the form of salt water is a major contaminant of groundwater, percolating through landfill liners and causing corrosion of steel.¹⁸ In soil typical levels are 100 ppm, and chloride levels in the oceans are about 0.5 M.

Fluoride concentrations can be determined by ^{19}F analysis or the specific ion electrode method.^{19,20} These systems, although well established, possess some disadvantages. The latter is a membrane electrode containing single crystals of LaF_3 , a method which is accurate but fragile and time-consuming.²¹ ^{19}F NMR spectroscopy can only be used reliably on the micromolar scale typical to most NMR spectroscopic studies. Neither system can be used to study biological processes in vivo, alternative systems allowing intracellular monitoring would be infinitely preferable to researchers.

Fluoride sensors have attracted a lot of research attention over recent years, many exploiting the interaction of Lewis acidic boron with fluoride or hydrogen bonding interactions.

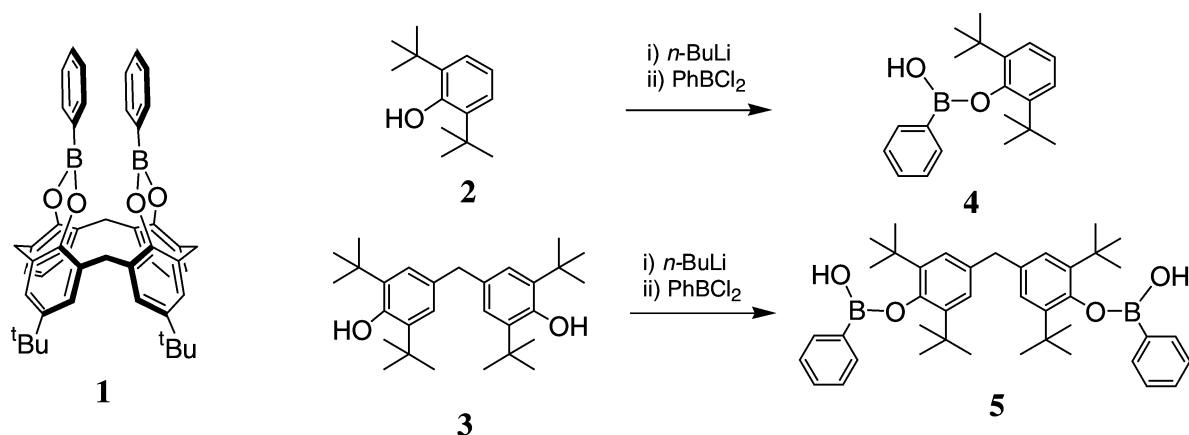
Sessler et al. have reported a number of fluoride sensors based on pyrrole hydrogen bond donors,^{22–24} as well as off the shelf fluoride sensors consisting of amides, amines, and phenols.²⁵ Smith et al. have also used phenol based receptors as hydrogen bond donors.²⁶

Boron forms trivalent, trigonal planar complexes such as $\text{B}(\text{OMe})_3$ and BF_3 . The characteristic empty 2p orbital at the boron center controls the Lewis acidic chemistry of boron.^{27–28} Boron centered fluoride receptors were first studied by Katz, who trapped fluoride ions between two electron accepting boron atoms in 1,8 naphthalendiyldibis-(dimethylborane).²⁹ The bridging was confirmed by the presence of large $^{19}\text{F}-^1\text{H}_{\text{Me}}$ coupling.

Our group were the first to use fluorescence to detect fluoride binding events.³¹ Excellent selectivity in aqueous solution at pH 5.5 was obtained using very simple boronic acids. Kubo et al. has developed a novel sensor system in which anions induce self-organization of phenyl boronic acids and alizarin. In the presence of fluoride or acetate ions, the three components (alizarin, boronic acid, and the anion) self-assemble switching "on" the fluorescence.^{32–34}

- (9) He, H. R.; Mortellaro, M. A.; Leiner, M. J. P.; Young, S. T.; Fraatz, R. J.; Tusa, J. K. *Anal. Chem.* **2003**, *75*, 549–555.
- (10) Schlebusch, H.; Paffenholz, I.; Zerback, R.; Leinberger, R. *Clin. Chim. Acta* **2001**, *307*, 107–112.
- (11) Kirk, L. K. *Biochemistry of the Halogens and Inorganic Halides*; Plenum Press: New York, 1991.
- (12) Kleerekoper, M. *Endocrinol. Metabol. Clin. North Amer.* **1998**, *27*, 441.
- (13) Briancon, D. *Rev. Rhum.* **1997**, *64*, 78–81.
- (14) Michigami, Y.; Kuroda, Y.; Ueda, K.; Yamamoto, Y. *Anal. Chim. Acta* **1993**, *274*, 299–302.
- (15) Xu, S.; Chen, K. C.; Tian, H. *J. Mater. Chem.* **2005**, *15*, 2676–2680.
- (16) Sohn, H.; Letant, S.; Sailor, M. J.; Trogler, W. C. *J. Am. Chem. Soc.* **2000**, *122*, 5399–5400.
- (17) Zhang, S. W.; Swager, T. M. *J. Am. Chem. Soc.* **2003**, *125*, 3420–3421.

- (18) Cosentino, P.; Grossman, B.; Shieh, C.; Doi, S.; Xi, H.; Erbland, P. *J. Geotech. Geoenviron. Eng.* **1995**, *121*, 610–617.
- (19) Konieczka, P.; Zygmunt, B.; Namiesnik, J. *Bull. Environ. Contam. Tox.* **2000**, *64*, 794–803.
- (20) Itai, K.; Tsunoda, H. *Clin. Chim. Acta* **2001**, *308*, 163–171.
- (21) Frant, M. S.; Ross, J. W. *Science* **1966**, *154*, 1553.
- (22) Black, C. B.; Andrioletti, B.; Try, A. C.; Ruiperez, C.; Sessler, J. L. *J. Am. Chem. Soc.* **1999**, *121*, 10438–10439.
- (23) Anzenbacher, P.; Try, A. C.; Miyaji, H.; Jursikova, K.; Lynch, V. M.; Marquez, M.; Sessler, J. L. *J. Am. Chem. Soc.* **2000**, *122*, 10268–10272.
- (24) Mizuno, T.; Wei, W. H.; Eller, L. R.; Sessler, J. L. *J. Am. Chem. Soc.* **2002**, *124*, 1134–1135.
- (25) Miyaji, H.; Sessler, J. L. *Angew. Chem., Int. Ed.* **2001**, *40*, 154–157.
- (26) Winstanley, K. J.; Sayer, A. M.; Smith, D. K. *Org. Biomol. Chem.* **2006**, *4*, 1760–1767.
- (27) Fenwick, J. T. F.; Wilson, J. W. *J. Chem. Soc., Dalton Trans.* **1972**, 1324–1326.
- (28) Jacobson, S.; Pizer, R. *J. Am. Chem. Soc.* **1993**, *115*, 11216–11221.
- (29) Worm, K.; Schmidtchen, F. P.; Schier, A.; Schafer, A.; Hesse, M. *Angew. Chem. Int. Ed. Engl.* **1994**, *33*, 327–329.
- (30) Katz, H. E. *J. Org. Chem.* **1985**, *50*, 5027–5032.
- (31) Cooper, C. R.; Spencer, N.; James, T. D. *Chem. Commun.* **1998**, 1365–1366.

Scheme 1. Structure of **1** (Rear Tertiary Butyl Groups Removed for Clarity) and Preparation of **4** and **5** from **2** and **3**

Gabbaï et al. have used a diboron species to bind fluoride and create a UV-based colorimetric sensor which is not affected by the presence of water. The association with the fluoride ion is higher than that observed with monofunctional borane receptors.³⁵ The same group have also utilized mercury for its ability to induce phosphorescence of hydrocarbon chromophores in a heteronuclear mercury–boron bidentate Lewis-acid species.³⁶ The naphthalene backbone enforces the proximity of the two Lewis-acid centers, leading to a higher binding constant than with Mes₃B, confirming cooperativity between the two Lewis acid species.

There are far fewer selective chloride sensors in the literature. Zhang has developed a reversible and accurate system for chloride levels in diluted serum samples, but the sensor suffers from interference from salicylate.³⁷ The sensor is bound to a polymer film, providing an example of the potential of such systems for “real-world” applications. Duan and Meng have reported a tris benzoimidazolium as a fluorescent chemosensor for chloride.³⁸ Diamond et al. have developed a tetrasubstituted calix[4]arene which displays chloride selective excimer quenching.³⁹ The chloride ions are thought to bind to the urea protons in the cavity, forcing the pyrene units apart.

Results and Discussion

Synthesis of Arylboronates 4 and 5. Our previous work has shown that the bis(bora)calix[4]arene **1** acts as a sensor for tetra-*n*-butylammonium fluoride (TBAF) in chloroform.⁴¹ To probe the factors affecting fluoride binding we decided to prepare a range of structurally related boronates. Com-

pound **1** was prepared using organoboron derivatization of a tetralithiated 4-*t*-butylcalix[4]arene,⁴⁰ and a similar protocol was used for preparation of compounds **4** and **5** (Scheme 1). *n*-Butyllithium was added dropwise to a solution of the starting phenol in toluene. After heating overnight at 100 °C, the resulting mixture was cooled and dichlorophenylborane was added. Following subsequent washing with water, **4** and **5** were afforded in good yields.

Structural Characterization of Arylboronates 4 and 5. Crystals of **4** were obtained by slow evaporation of a supersaturated hexane solution, and the structure was determined by X-ray crystallography (Figure 1). The molecular structure of arylboronate **4** is as expected. On the supramolecular level, dimeric association occurs via intermolecular hydrogen bonding interactions between two molecules of **4**. A short O–H⋯O hydrogen bond [O(3)–H(3)⋯O(1); H⋯O distance, 2.03(3) Å, O⋯O distance, 2.864(2) Å, O–H⋯O angle, 160(2) °] is accompanied by a O–H⋯π interaction in which the O(1)–H(1) vector is directed at the face of the aryl ring [O(1)–H(1)⋯X, where X = centroid of C(51)–C(56); H⋯X distance, 2.53(2), O⋯X distance, 3.190(1) Å].

A single crystal of **5** was obtained via slow evaporation from toluene, and the molecular structure elucidated by X-ray diffraction. In **5**·H₂O, the aryl rings adopt a “butterfly” conformation (approximate C_{2v} symmetry). Other features of the molecular structure are as expected. The supramo-

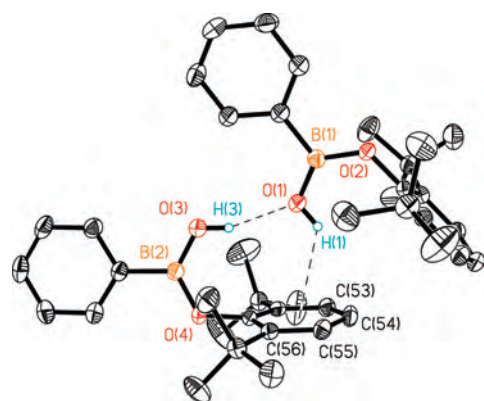


Figure 1. Molecular structure of **4** showing O–H⋯O and O–H⋯π interactions between the two independent molecules of the asymmetric unit.

- (32) Kubo, Y.; Ishida, T.; Kobayashi, A.; James, T. D. *J. Mater. Chem.* **2005**, *15*, 2889–2895.
 (33) Kubo, Y.; Ishida, T.; Minami, T.; James, T. D. *Chem. Lett.* **2006**, *35*, 996–997.
 (34) Kubo, Y.; Kobayashi, A.; Ishida, T.; Misawa, Y.; James, T. D. *Chem. Commun.* **2005**, 2846–2848.
 (35) Chiu, C. W.; Gabbai, F. P. *J. Am. Chem. Soc.* **2006**, *128*, 14248–14249.
 (36) Melaimi, M.; Gabbai, F. P. *J. Am. Chem. Soc.* **2005**, *127*, 9680–9681.
 (37) Zhang, W.; Rozniecka, E.; Malinowska, E.; Parzuchowski, P.; Meyerhoff, M. E. *Anal. Chem.* **2002**, *74*, 4548–4557.
 (38) Bai, Y.; Zhang, B. G.; Xu, J.; Duan, C. Y.; Dang, D. B.; Liu, D. J.; Meng, Q. *New J. Chem.* **2005**, *29*, 777–779.
 (39) Schazmann, B.; Alhashimy, N.; Diamond, D. *J. Am. Chem. Soc.* **2006**, *128*, 8607–8614.

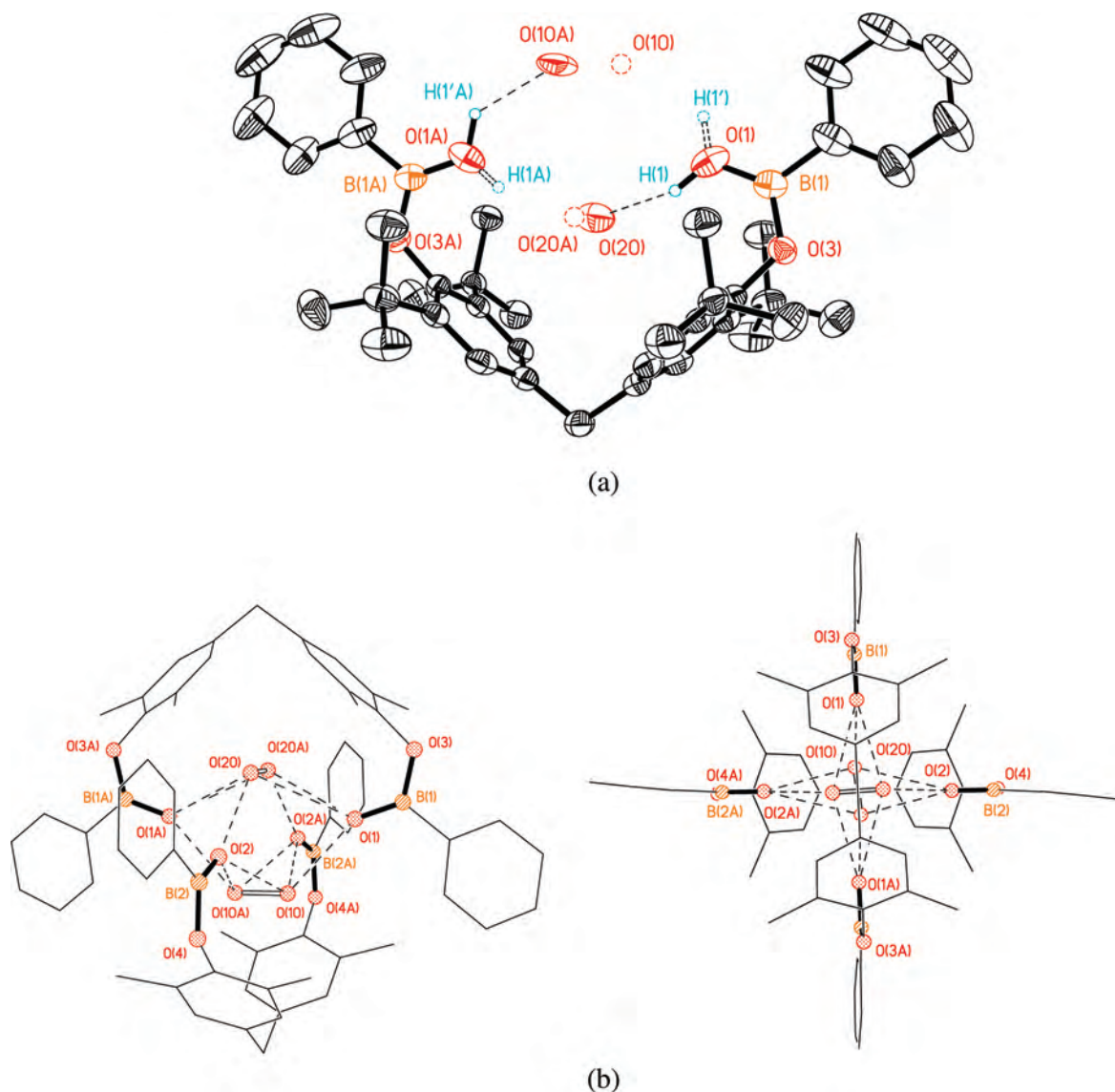


Figure 2. Molecular structure of $5 \cdot \text{H}_2\text{O}$: (a) One arylboronate unit highlighting the 50:50 disorder of the B–OH and H_2O groups (H atoms of the disordered H_2O not located in the X-ray structure, H atoms other than those involved in H-bonding omitted for clarity, thermal ellipsoids at the 50% probability level); (b) the dimeric structure highlighting the H_2O -filled cavity generated by the two orthogonal arylboronate units (all H atoms omitted for clarity and dashed lines between O atoms identifying short ($<3.2 \text{ \AA}$) $\text{O} \cdots \text{O}$ distances and probable $\text{O} - \text{H} \cdots \text{O}$ hydrogen bond interactions).

lecular structure consists of two orthogonal molecules of **5** assembled around two water molecules. In the solid state, disorder of the hydrogen atoms of the B–OH and H_2O units precludes detailed analysis of the hydrogen bonding interactions involved (Figure 2).

Subsequently, crystals of **5** were also grown under rigorously anhydrous conditions. In the absence of water, **5** adopts a “propeller” conformation of approximate C_2 symmetry (Figure 3a) and associates into a two-dimensional supramolecular array via a series of $\text{O} - \text{H} \cdots \pi$ interactions (Figure 3b,c).⁴¹

Colorimetric Response to Fluoride of Phenols (2 and 3) and Arylboronates (4 and 5). On addition of an excess of TBAF to solutions of **4** or **5** in chloroform dramatic color

changes from colorless to yellow (**4**) or purple (**5**) are observed. In both cases, NMR spectroscopic analysis clearly indicates TBAF-mediated cleavage of the boron-aryloxy bond, an observation in agreement with a recent report by Bresner et al.⁴² These observations led us to investigate the addition of fluoride to the parent phenols **2** and **3**, and they also exhibited similar color changes to those observed with **4** and **5** (Figure 4). In the light of the similar behavior of both phenols and arylboronates in the presence of fluoride, a feasible mechanism for this colorimetric response involves a common phenolate anion intermediate obtained via either fluoride-mediated deboronation or deprotonation, followed by ambient oxidation to a colored radical as shown in Scheme 2. Precedent for these mechanisms exists. For example, fluoride-mediated deprotonation of phenol-based

(40) Arimori, S.; Davidson, M. G.; Fyles, T. M.; Hibbert, T. G.; James, T. D.; Kociok-Köhn, G. I. *Chem. Commun.* **2004**, 1640–1641.

(41) Broder, C. K.; Davidson, M. G.; Forsyth, V. T.; Howard, J. A. K.; Lamb, S.; Mason, S. A. *Cryst. Growth Des.* **2002**, 2, 163–169.

(42) Bresner, C.; Day, J. K.; Coombs, N. D.; Fallis, I. A.; Aldridge, S.; Coles, S. J.; Hursthouse, M. B. *Dalton Trans.* **2006**, 3660–3667.

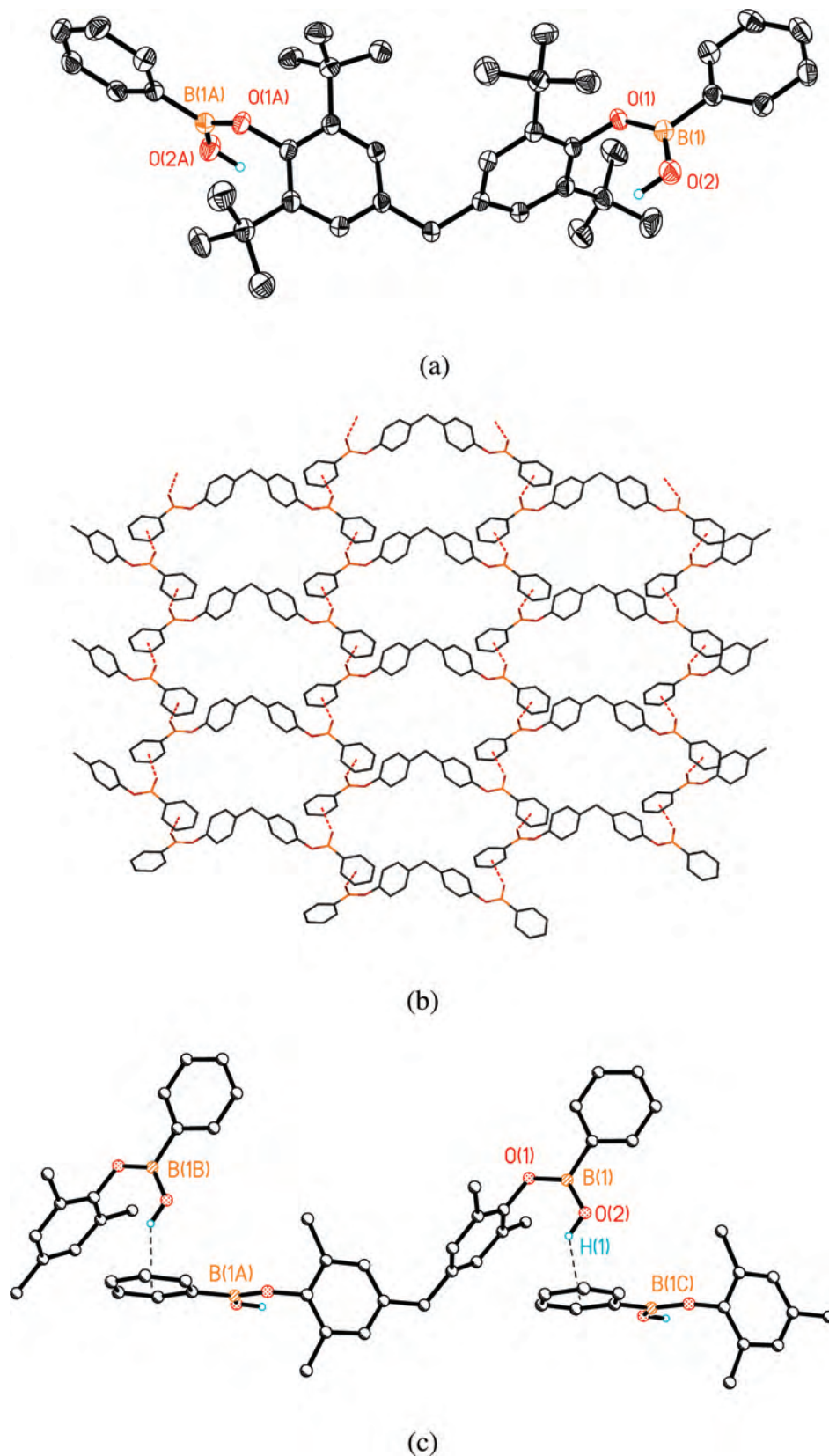


Figure 3. (a) Molecular structure of **5**. H atoms other than those of B–OH omitted for clarity, thermal ellipsoids at the 50% probability level; (b) the supramolecular structure of **5**; (c) details of intermolecular interactions in **5**. All H atoms other than those of B–OH omitted for clarity. Dashed lines between H atoms and centroid (X) identify short (2.46 Å) $\text{H}\cdots\pi$ distances with a O–H–X angle of 127° . Lattice toluene (C_7H_8) omitted for clarity.

anion sensors has been observed⁴³ (as has deprotonation of N–H groups of other anion sensors^{44–53}) and fluoride-

mediated deboronations are known.⁴² The colorimetric response of two viologen based anion hosts toward carboxy-

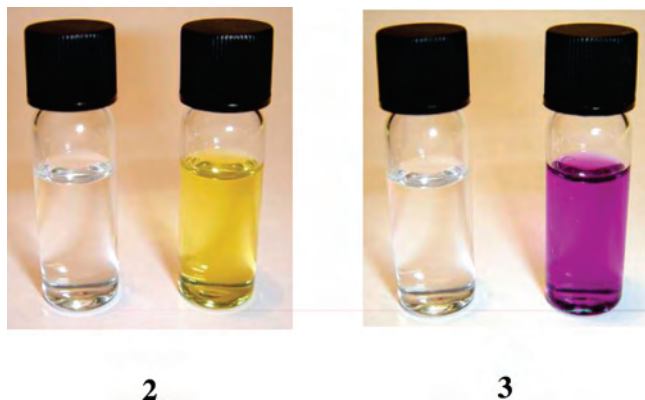


Figure 4. Colorimetric response of **2** and **3** (1 mM) to the addition of fluoride (5 mM) in dichloromethane after 30 s.

lates has also been shown to be due to the formation of viologen radicals.⁵⁴

To investigate the anion and radical formation (Scheme 2), electrochemical measurements were conducted on **5** using cyclic voltammetry and differential pulse voltammetry modes (Figure 5). In the absence of fluoride, a colorless solution of **5** (1.0 mM) in acetonitrile exhibits a chemically irreversible oxidation peak at 1.8 V versus SCE (see Figure 5i) at a boron-doped diamond electrode with wide potential window.⁵⁵ Addition of 0.2 mM TBAF immediately causes a decrease in the peak response at 1.8 V versus SCE and the appearance of a new peak at 1.5 V versus SCE, which can be tentatively assigned to the monofluoride adduct shown in Scheme 2. For TBAF concentrations of 0.4 mM and higher, two new peak responses at -0.3 V and $+0.1$ V versus SCE are observed, which can be assigned to the oxidation of the phenoxyl dianion to a colored phenoxyl diradical. In complementary cyclic voltammetry experiments (not shown) both peak responses are observed to be chemically irreversible. For applied potentials positive of about 0.0 V versus SCE the characteristic purple color of the phenoxyl diradical is observed at the electrode surface. Furthermore, additional experiments with the parent phenol **3** in the presence of

TBAOH show that the peaks observed at -0.3 V and $+0.1$ V versus SCE are associated with this phenoxyl dianion. Clearly the fluoride anions have removed the boronic acid residues and liberated phenoxyl dianion (Scheme 2), which in the presence of the electrode or dioxygen quickly undergoes multielectron oxidation to the colored diradical. The voltammetric peaks at -0.3 V and $+0.1$ V versus SCE may be regarded as diagnostic for fluoride. However, when tetra-*n*-butylammonium chloride (TBACl) is added to **5** (Supporting Information), no easy to oxidize fragments are formed and no color change is observed. Upon addition of chloride a new signal at 1.3 V versus SCE is detected, and this signal can be assigned to chloride oxidation.

UV spectroscopy was used to investigate the interaction of compound **3** in dichloromethane solution with various anions including F^- , Cl^- , Br^- , and $H_2PO_4^-$ as their tetra-*n*-butylammonium salts. The compound exhibited a dramatic response to fluoride with a new peak appearing at 580 nm. Figure 6 shows the extremely high selectivity against a range of common anions. No visible color change is apparent with the addition of any anion besides fluoride. Similar UV spectra were obtained for the addition of F^- , Cl^- , Br^- , and $H_2PO_4^-$ as their tetra-*n*-butylammonium salts to compound **5**.

The fluorescence spectrum of **5** in dichloromethane was recorded. The excitation spectrum showed two peaks, one at 251 nm and another one of lower energy at 289 nm. Exciting at 289 nm, a fairly intense emission peak is observed, with a maximum at 370 nm. As expected, after one equivalent of TBAF is added the fluorescence/the peak is almost completely quenched. Quenching of the fluorescence in this case is attributed to fluoride mediated deboronation (Scheme 2).

Fluorescence spectroscopy was then used to study the effect of chloride ion concentration on the fluorescence spectrum of **5** in CH_2Cl_2 (Figure 7).

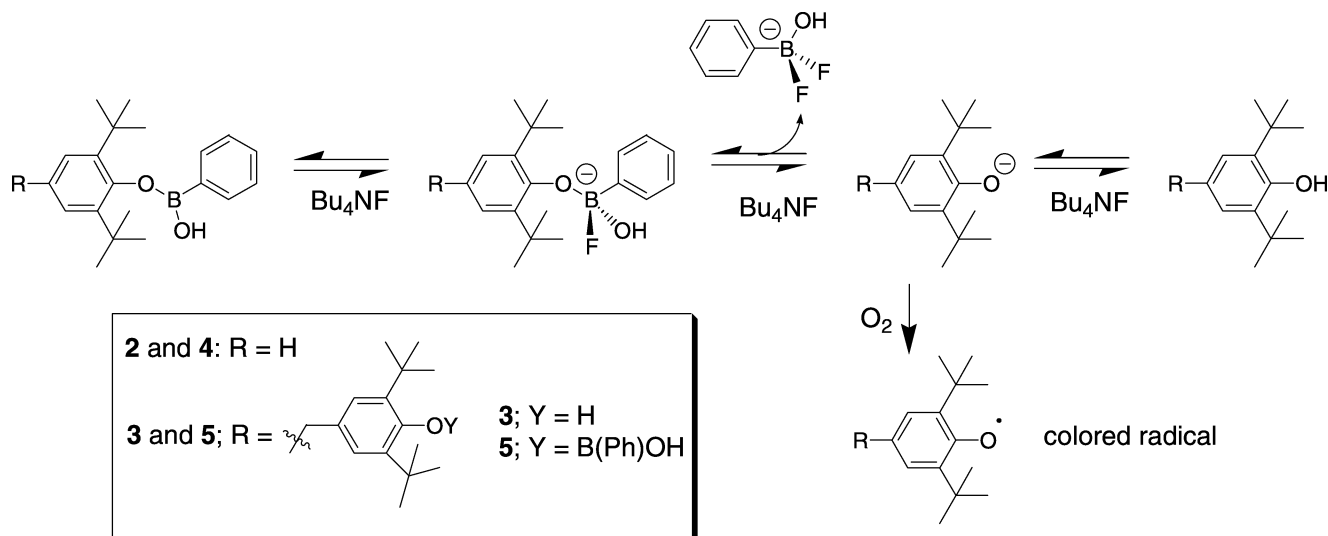
The quenching is nonlinear, and fits a 2:1 model with a $\log K = 4.5$. It is important to note that any model including a 1:1 complex does not fit the data, that is, a 1:1 model or a 1:1 and 2:1 mixed model (Figure 8).

We believe that addition of chloride causes a conformational change between the staggered “chicken-wire” structure shown in Figure 3 and a hydrogen bonded cavity as in Figure 2, with the chloride acting in a similar role to the water molecule (Figure 2) and forming hydrogen bonds with four B–OH moieties from two molecules of **5**. This conformational change affects the π systems of the two phenyl rings and hence the fluorescence intensity of the emission.

A similar titration was repeated with tetra-*n*-butylammonium (TBABr) bromide to probe the selectivity. At 10.0 mM halide ion, the relative intensity for chloride is 0.21 and for bromide 0.86.

The alcohol precursor **3** was also studied by fluorescence spectroscopy (1.0 mM). The compound was excited at 257 nm producing an emission peak at 308 nm, the intensity of which changes negligibly with increasing chloride concentration.⁵⁶ Addition of TBAF causes complete fluorescence quenching attributed to fluoride mediated deprotonation (Supporting Information). For the monoboronic acid system

- (43) Lee, K. H.; Lee, H.-Y.; Lee, D. H.; Hong, J.-I. *Tetrahedron Lett.* **2001**, *42*, 5447–5449.
- (44) Gunnlaugsson, T.; Kruger, P. E.; Jensen, P.; Tierney, J.; Ali, H. D. P.; Hussey, G. M. *J. Org. Chem.* **2005**, *70*, 10875–10878.
- (45) Camiolo, S.; Gale, P. A.; Hursthouse, M. B.; Light, M. E.; Shi, A. J. *Chem. Commun.* **2002**, 758–759.
- (46) Camiolo, S.; Gale, P. A.; Hursthouse, M. B.; Light, M. E. *Org. Biomol. Chem.* **2003**, *1*, 741–744.
- (47) Gunnlaugsson, T.; Kruger, P. E.; Jensen, P.; Pfeiffer, F. M.; Hussey, G. M. *Tetrahedron Lett.* **2003**, *44*, 8909–8913.
- (48) Costero, A. M.; Jose Banuls, M.; Jose Aurell, M.; Ward, M. D.; Argent, S. *Tetrahedron* **2004**, *60*, 9471–9478.
- (49) Boiocchi, M.; Del Boca, L.; Gomez, D. E.; Fabbri, L.; Licchelli, M.; Monzani, E. *J. Am. Chem. Soc.* **2004**, *126*, 16507–16514.
- (50) Esteban-Gomez, D.; Fabbri, L.; Licchelli, M. *J. Org. Chem.* **2005**, *70*, 5717–5720.
- (51) Boiocchi, M.; Del Boca, L.; Esteban-Gómez, D.; Fabbri, L.; Licchelli, M.; Monzani, E. *Chem.–Eur. J.* **2005**, *11*, 3097–3104.
- (52) Gomez, D. E.; Fabbri, L.; Licchelli, M.; Monzani, E. *Org. Biomol. Chem.* **2005**, *3*, 1495–1500.
- (53) Evans, L. S.; Gale, P. A.; Light, M. E.; Quesada, R. *Chem. Commun.* **2006**, 965–967.
- (54) Dickson, S. J.; Wallace, E. V. B.; Swinburne, A. N.; Paterson, M. J.; Lloyd, G. O.; Beeby, A.; Belcher, W. J.; Steed, J. W. *New J. Chem.* **2008**, in press.
- (55) Compton, R. G.; Foord, J. S.; Marken, F. *Electroanalysis* **2003**, *15*, 1349–1363.

Scheme 2. Fluoride-Mediated Deboronation (4 or 5) or Deprotonation (2 or 3) Followed by Atmospheric Oxidation to a Colored Radical

4 excitation at 251 nm produced a weaker fluorescence emission at 308 and 330 nm, the intensity of which changes negligibly with increasing chloride concentration. Addition of TBAF causes fluorescence quenching attributed to fluoride mediated deboronation (Supporting Information). These results clearly indicate that the two boronate functionalities of **5** are required for fluorescence quenching by chloride ions.

Experimental Section

General Procedures. Solvents and Reagents. Solvents and reagents were reagent grade unless stated otherwise and were purchased from Frontier Scientific Europe Ltd., Lancaster Synthesis Ltd. and Sigma-Aldrich Company Ltd. and were used without further purification, unless stated otherwise.

Nuclear Magnetic Resonance Spectra. Nuclear magnetic resonance spectra were run in chloroform- D . 1H , ^{11}B , and ^{13}C spectra were measured using a Bruker AVANCE 300 spectrometer.

1H spectra were recorded at 300.22 MHz, ^{11}B spectra at 96.32 MHz, and $\{^1H\}^{13}C$ at 75.50 MHz. Chemical shifts (δ) are expressed in parts per million and are reported relative to the residual solvent peak or to tetramethylsilane as an internal standard in 1H and $\{^1H\}^{13}C$ spectra. Chemical shifts (δ) are expressed in parts per million and are reported relative to boron trifluoride diethyl etherate as an external standard in ^{11}B spectra. The multiplicities and general assignments of the spectroscopic data are denoted as singlet (s), doublet (d), triplet (t), quartet (q), quintet (quin), doublet of doublets (dd), doublet of doublets of doublets (ddd), doublet of triplets (dt), triplet of triplets (tt), unresolved multiplet (m), apparent (app), broad singlet (bs), and aryl (Ar).

Mass Spectra. Mass spectra were recorded by the EPSRC National Mass Spectrometry Service Centre, Swansea. Electron impact (EI) and chemical ionization (CI) analyses were performed in positive ionization mode. Low resolution EI and CI measurements were performed on a Micromass Quattro II triple quadrupole instrument, with ammonia as the CI reagent gas. Electrospray

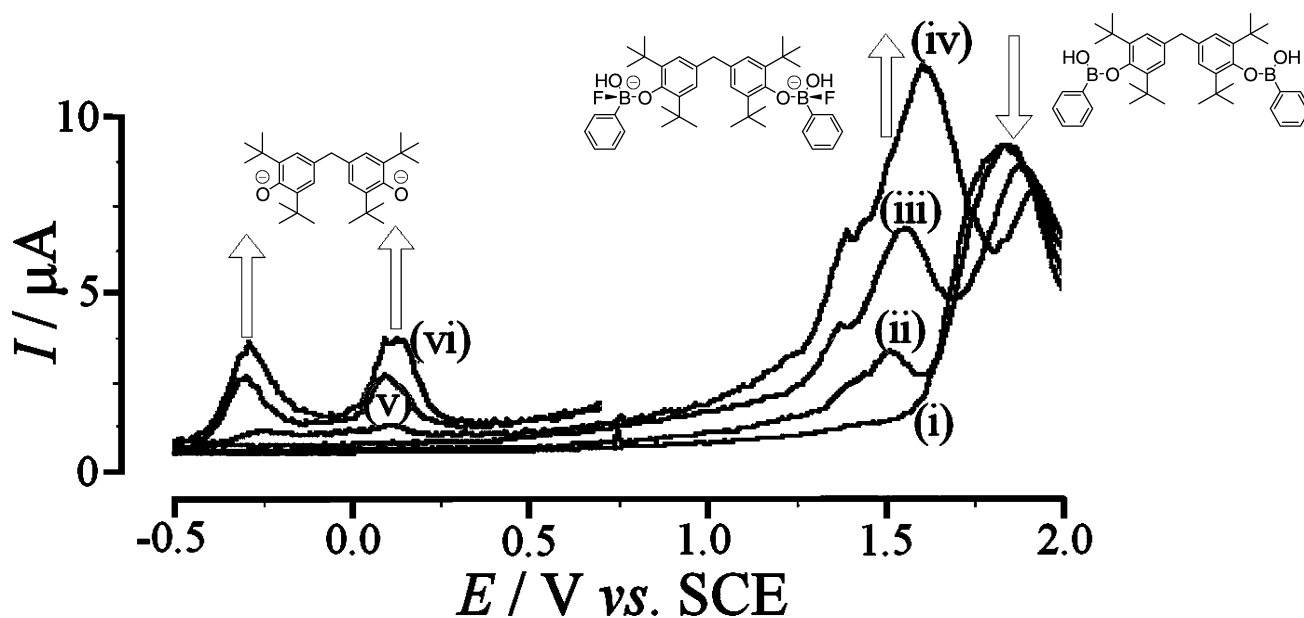


Figure 5. Differential pulse voltammograms (modulation time 0.05 s, modulation amplitude 25 mV) for the oxidation of 1.0 mM **5** in acetonitrile (0.1 M NBu_4PF_6) at a 3 mm diameter boron-doped diamond electrode in the presence of (i) 0 mM, (ii) 0.2 mM, (iii) 0.4 mM, (iv) 0.6 mM, (v) 0.8 mM, and (vi) 1.0 mM fluoride.

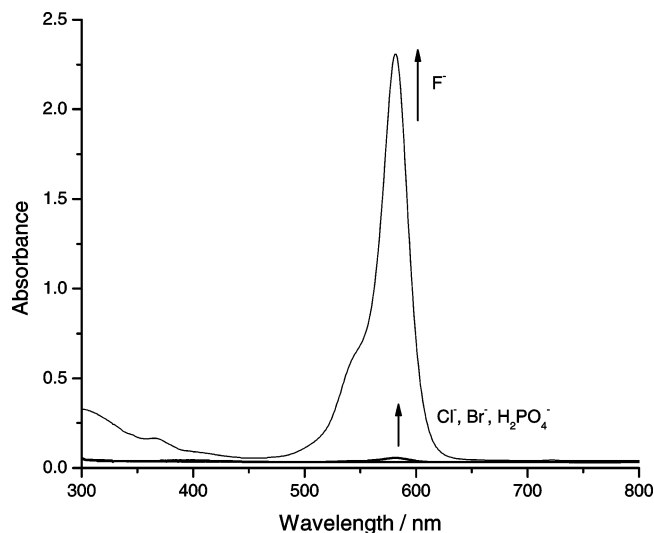


Figure 6. UV spectra of **3** in dichloromethane (0.1 mM for F^- and 1.0 mM for Cl^- , Br^- , and $H_2PO_4^-$) upon addition of F^- (0.5 mM), Cl^- (5 mM), Br^- (5 mM), and $H_2PO_4^-$ (5 mM) as tetra-*n*-butylammonium salts.

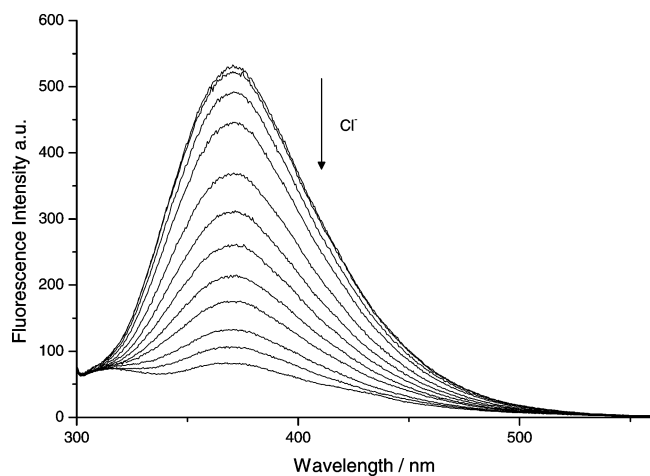


Figure 7. Fluorescence spectra of **5** in dichloromethane (1.0 mM, λ 289 nm) with increasing concentration of chloride (0–15.0 mM).

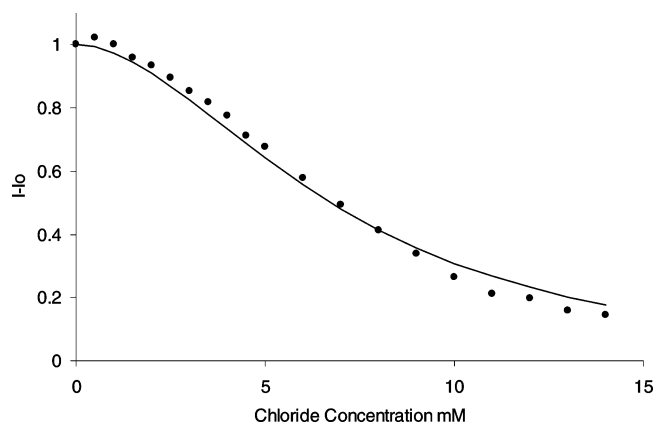


Figure 8. Plot illustrating the quenching action of increasing concentration of chloride on the fluorescence of **5**.

ionization measurements were performed in both positive and negative ionization modes (ES^+ and ES^- respectively). For low resolution measurements the sample was loop injected into a stream of 1:1 methanol/dichloromethane, on a Waters ZQ4000 single quadrupole mass spectrometer or Mariner API-TOF with reflectron detector mass spectrometer. High resolution EI, CI, ES^+ , and ES^-

measurements were conducted on either a Finnigan MAT95 high resolution double focusing mass spectrometer or a MAT900 high resolution double focusing mass spectrometer with tandem ion trap. For EI and CI measurements heptacosane (perfluorotributylamine) was used as the reference compound. Both low and high resolution fast atom bombardment (FAB or liquid secondary ion mass spectrometry, LSIMS) analyses were performed, in positive or negative ionization mode, on either a Finnigan MAT95 high resolution double focusing mass spectrometer or a MAT900 high resolution double focusing mass spectrometer with tandem ion trap, using meta-nitrobenzyl alcohol (NBA) as the matrix liquid.

Elemental Analyses. Elemental analyses were performed by the Department of Chemistry, University of Bath, using an Exeter Analytical Inc. CE-440 elemental analyzer.

Melting Points. Capillary melting points were determined using a Büchi 535 melting point apparatus. The readings were taken from a mercury-in-glass thermometer and are reported uncorrected as the meniscus point (unless stated otherwise), rounded to the nearest $1^\circ C$ with a heating ramp rate of $0.5^\circ C\ min^{-1}$. In instances where a reproducible liquid meniscus could not be obtained, the onset point (onset) was recorded instead and is noted. Where the sample changed color or evolved gas during or after the melt, thermal decomposition (dec) is noted.

Fluorescence Measurements. Fluorescence measurements were performed on a Perkin-Elmer luminescence spectrophotometer LS 50B, utilizing Starna Silica (quartz) cuvettes with 10 mm path lengths, four faces polished. Data was collected via the Perkin-Elmer FL Winlab software package. All solvents used in fluorescence measurements were HPLC or Fluorescence grade and the water was deionized.

Electrochemical Measurements. Voltammetric and differential pulse voltammetric data were obtained with a microAutolab III system (Ecochemie) and in a conventional three-electrode cell. The counter and reference electrodes were platinum gauze and a saturated calomel electrode (SCE), respectively. A 3 mm diameter boron-doped diamond disk electrode was obtained from Windsor Scientific (Slough, U.K.). All measurements were conducted under argon (BOC, U.K.) and at $20 \pm 2^\circ$.

Single Crystal Preparation and Crystallographic Methods. Single crystals were obtained by dissolving the compounds in hexane or toluene. Good quality crystals were obtained overnight. Crystallographic data for **4** and **5** are available as Supporting Information. Data were collected on a Nonius KappaCCD diffractometer. Structure solution was performed using SHELX86⁵⁷ and refinement was by full-matrix least-squares on F^2 using SHELX97 software. Selected data is shown in Table 1.

Synthesis (2,6-Di-*tert*-butylphenyl)hydrogenphenylboronate. 2,6-Di-*tert*-butylphenol (1.00 g, 4.85 mmol) was dissolved in dry toluene (40 mL) and stirred in a nitrogen atmosphere. *N*-butyllithium (1.6 mM in hexanes, 3.33 mL, 5.33 mmol) was added dropwise by syringe and the mixture heated at $100^\circ C$ overnight. After cooling the reaction to RT, dichlorophenylborane ($700\ \mu L$, 5.33 mmol) was introduced and heating continued for a further 18 h. The white precipitate dissolved in the subsequent thrice washing with water ($3 \times 60\ mL$), and after drying over $MgSO_4$ and the solvent removed in vacuo, an off-white solid was obtained (1.366 g, 91%); δ_H (300 MHz, $CDCl_3$, Me_4Si) 1.31 (s, 18H, $C(CH_3)_3$), 4.07 (bs, 1H, B–OH), 6.98 (1H, t, $3J_{HH}$ 7.5, Ar–H), 7.28 (2H, d, $3J_{HH}$ 7.9, Ar–H), 7.43

(56) Smith, D. K. *Org. Biomol. Chem.* **2003**, *1*, 3874–3877.

(57) Sheldrick, G. M. *SHELX-86, Computer Program for Crystal Structure Determination*; University of Göttingen: Göttingen, Germany, 1986.

(58) Sheldrick, G. M. *SHELX-97, Computer Program for Crystal Structure Refinement*; University of Göttingen: Göttingen, Germany, 1997.

Table 1. Summary of Crystallographic Data for Compounds **4** and **5**

	4	5·H₂O	5·C₇H₈
empirical formula	C ₂₀ H ₂₇ BO ₂	C ₄₁ H ₅₆ B ₂ O ₅	C ₄₈ H ₆₂ B ₂ O ₄
formula weight	310.23	650.48	724.60
crystal color	colorless	colorless	colorless
crystal size, mm	0.20 × 0.20 × 0.10	0.10 × 0.10 × 0.05	0.25 × 0.13 × 0.13
crystal system	monoclinic	monoclinic	monoclinic
space group	<i>P2₁/a</i>	<i>C2/c</i>	<i>C2/c</i>
<i>a</i> , Å	12.0120(1)	19.1590(3)	26.7710(6)
<i>b</i> , Å	14.4200(1)	21.4040(3)	8.6100(2)
<i>c</i> , Å	21.9640(2)	19.1280(6)	18.6130(5)
α, deg	105.101(1)	90.674(1)	95.412(1)
<i>V</i> , Å ³	3673.08(5)	7843.5(3)	4271.1(2)
<i>Z</i>	8	8	4
<i>T</i> , K	150(2)	150(2)	150(2)
<i>D</i> _{calc} , g cm ⁻³	1.122	1.102	1.127
μ, mm ⁻¹	0.069	0.070	0.069
λ, Å	0.71073 (Mo Kα)	0.71073 (Mo Kα)	0.71073 (Mo Kα)
2θ _{max} , deg	52	52	56
GOF (<i>F</i> ²)	1.042	1.005	1.023
<i>R</i> ₁ [<i>I</i> > 2σ(<i>I</i>)]	0.0474	0.0609	0.0555
w <i>R</i> ₂ (all data, <i>F</i> ²)	0.1186	0.1592	0.1683

(3H, m, Ar-*H*), 7.95 (2H, ddd, ³*J*_{HH} 1.5, ³*J*_{HH} 3.0, ³*J*_{HH} 6.8, Ar-*H*); δB (96 MHz, CDCl₃) 20.0; *m/z* (CI⁺) found 310.2099 [M]⁺. Expected value for C₂₀H₂₇O₂B 310.2423.

Bis(3,5-di-*tert*-butyl-4(hydrogenphenylboronoxy)phenyl)methane. 4,4'-Methylenebis(2,6-di-*tert*-butylphenol) (1.00 g, 2.35mmol) was dissolved in 40 mL dry toluene under nitrogen. During rapid stirring, *N*-butyllithium (1.6 M in hexanes, 4.95 mmol, 3.09 mL) was added dropwise and the mixture heated at 100 °C overnight. Upon cooling, dichlorophenylborane (680 μL, 5.18 mmol) was added and heating at 100 °C reinitiated for an additional 12 h. The resulting white suspension was washed three times with water (60 mL), dried over MgSO₄, and the solvent removed in vacuo to afford a yellow oil. Recrystallization gave the title compound as an off-white powder (1.250 g, 84%); mp 162–164 °C (dec); δH (300 MHz, CDCl₃, Me₄Si) 1.29 (36H, s, Ar-(CH₃)₃), 3.88 (2H, s, Ar-CH-Ar'), 7.11 (4H, s, Ar-*H*), 7.41 (6H, m, Ar-*H*), 7.94 (4H, s, Ar-*H*); δC (75 MHz, CDCl₃, Me₄Si) 32.02, 35.93, 42.22, 127.06, 128.77, 131.88, 135.31, 136.12, 142.26, 148.88; δB (96 MHz, CDCl₃) 20.0; *m/z* (method of ionization) 650.4546 [M + NH]⁺. The calculated mass of C₄₁H₅₄B₂O₄.NH₄⁺ is 650.4546.

Elemental Analysis. Expected C = 77.86%, H = 8.61% for C₄₁H₅₄B₂O₄. Found C = 77.80%, H = 8.63% (average of two measurements).

Conclusions

A range of substituted phenols were tested for colorimetric responses to fluoride and other anions in solution. Several compounds were found to selectively deprotonate in the presence of fluoride ions and form a highly colored and stable radical species. Thus, simple, commercially available substrates have been shown to act as colorimetric sensors for fluoride. We envision these simple molecules being employed

in sensor materials, where a one off response to the presence of fluoride is required. For example, early warning badges to report the release of fluoride containing nerve agents such as sarin.^{16,17}

The phenols **2** and **3** described above were converted into aryl boronates **4** and **5**, where **5** has been found to act as a fluorescent sensor for chloride ions in dichloromethane. Since only compound **5** displays this fluorescence response, we propose that the chloride ion is hydrogen bonding to both BOH groups in **5**. This is a similar binding motif to that observed in the crystal structure of **5·H₂O** (Figure 2).

Our group is currently developing chloride receptors based on the general structure of **5·H₂O** that are stable to fluoride and work under aqueous conditions.

Acknowledgment. T.D.J. and E.G. wish to acknowledge the University of Bath and Beckman-Coulter for support.

Note Added after ASAP Publication. There was a reformat of references in the version published ASAP May 28, 2008; the corrected version published ASAP June 4, 2008.

Supporting Information Available: Figures with UV and fluorescence spectra of **2–5** (PDF) and CIF files for **4**, **5·H₂O**, and **5·C₇H₈**. This material is available free of charge via the Internet at <http://pubs.acs.org>.

IC800204Q